An exact solution for free vibration of thin functionally graded rectangular plates

A Hasani Baferani[1]**, A R Saidi**[1*]**,** and **E Jomehzadeh**[2]

[1]Department of Mechanical Engineering, Shahid Bahonar University of Kerman, Kerman, Iran

[2]Shahid Bahonar University of Kerman, Young Researchers Society, Kerman, Iran

The manuscript was received on 30 December 2009 and was accepted after revision for publication on 15 June 2010.

DOI: 10.1243/09544062JMES2171

Abstract: The aim of this article is to find an exact analytical solution for free vibration characteristics of thin functionally graded rectangular plates with different boundary conditions. The governing equations of motion are obtained based on the classical plate theory. Using an analytical method, three partial differential equations of motion are reformulated into two new decoupled equations. Based on the Navier solution, a closed-form solution is presented for natural frequencies of functionally graded simply supported rectangular plates. Then, considering Levy-type solution, natural frequencies of functionally graded plates are presented for various boundary conditions. Three mode shapes of a functionally graded rectangular plate are also presented for different boundary conditions. In addition, the effects of aspect ratio, thickness–length ratio, power law index, and boundary conditions on the vibration characteristics of functionally graded rectangular plates are discussed in details. Finally, it has been shown that the effects of in-plane displacements on natural frequencies of functionally graded plates under different boundary conditions have been studied.

Keywords: free vibration, functionally graded material, rectangular plate, exact solution, Levy solution, Navier solution

1 INTRODUCTION

Functionally graded materials (FGMs) are new microscopically inhomogeneous materials in which the mechanical properties vary smoothly and continuously from one surface to the other [**1–4**]. The concept of FGM was first proposed in 1984 by the material scientists in the Sendai area of Japan. Typically, these materials are made from a mixture of metal and ceramic, or a combination of different metals. They are high-performance heat-resistant materials that are able to withstand the ultra-high temperature and the extremely large thermal gradients. FGMs are used in the industry extensively. For example, they are used as thermal barriers in aerospace missiles in which the ceramic face of the plate is exposed to high temperature.

Many researches for static and dynamic analyses of FG plates are available in the literature. Yang and Shen [**5**] investigated dynamic response of initially stressed functionally graded (FG) rectangular thin plates. Some studies developed the meshless method for static and dynamic analyses of FG elastic rectangular plates [**6–9**]. He *et al.* [**10**], by using the finite-element method, investigated the active control of FG plates with integrated piezoelectric sensors and actuators. There are some three-dimensional (3D) solutions for free vibration analysis of FG rectangular plates in the literature. For example, Vel and Batra [**11**] presented an analytical 3D solution for free vibration of simply supported rectangular plates. Also, 3D vibration analysis of FG plates was studied using the numerical methods by some researchers [**12, 13**]. Kim [**14**] presented temperature-dependent vibration analysis of FG rectangular plates. The frequency equation was solved using the Rayleigh–Ritz procedure based on the third-order shear deformation plate theory. Matsunaga [**15**] performed free vibration and stability of FG plates according to a 2D higher-order deformation theory. Zhang and Zhou [**16**] analysed FG thin plates based on

Corresponding author: Department of Mechanical Engineering, Shahid Bahonar University of Kerman, Jomhouri Blvd, Kerman, Iran.

email: saidi@mail.uk.ac.ir; a_r_saidi@yahoo.com

the concept of physical neutral surface. They defined a new physical neutral surface and, by using this surface, non-linear equations were obtained. Fares *et al.* [17] performed the efficient and simple refined theory for bending and vibration of FG plates. Hosseini-Hashemi *et al.* [18] studied the free vibration of FG rectangular plates using first-order shear deformation plate theory. They neglected the effects of in-plane displacement on free vibration of rectangular plates. Zhao *et al.* [19] performed free vibration analysis of FG plates using the element-free *kp-Ritz* method. Using the classical plate theory, Liu *et al.* [20] studied the free vibration of FG rectangular plates by assuming the in-plane variation of material properties of the plate in which the bending/stretching equations are not coupled.

It is more convenient to use the decoupled form of governing equations for solving the mechanical analysis of the plates. For free vibration analysis, Jomehzadeh and Saidi [21, 22] decoupled the governing equations of motion of transversely isotropic sectorial and annular sector plates. The decoupling of bending–stretching governing equations of FG rectangular plates was first investigated by Saidi and Jomehzadeh [23]. Also, Mohammadi *et al.* [24, 25] presented a decoupling method for buckling analysis of thin and moderately thick FG rectangular plates with two opposite edges simply supported.

Most of the works concerning the analytical solution for vibration of FG plates are limited to all edges of simply supported plates. Also, some studies presented Levy solution for free vibration of FG plates without considering the in-plane displacements [18, 20]. To the best of authors' knowledge, there is no work in the literature on analytical solution for vibration of FG plates with considering the effect of in-plane displacements.

In the present article, an exact analytical solution for free vibration of thin FG rectangular plates is presented based on classical plate theory and the effects of in-plane displacement on the vibration of FG rectangular plates are studied. By using an analytical method, the coupled equations of motion are decoupled. A closed-form solution for finding the natural frequencies of FG simply supported rectangular plates is presented. Also, a Levy-type solution is presented for FG plates that have simply supported boundary conditions in x-direction and arbitrary boundary conditions at the edges in y-direction. Finally, the effects of aspect ratio, thickness–length ratio, power law index, and boundary conditions on the vibration characteristics of FG rectangular plates are discussed in details. The novelty of this work is that all terms in the governing equations are considered and no simplification is done for finding and solving the governing equations. It has been shown that the in-plane displacements have significant effects on natural frequencies of FG rectangular plates and cannot be neglected.

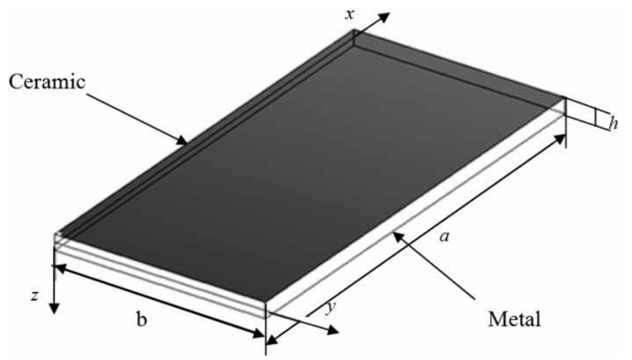

Fig. 1 Geometry and coordinate of FG rectangular plate

2 GOVERNING EQUATION

Here, an FG rectangular plate of length a, width b, and thickness h is considered. The geometry of the plate and the coordinate system are shown in Fig. 1. It is assumed that the properties of FG plate vary smoothly and continuously through the thickness from the ceramic surface to metal surface. $E(z)$ is Young modulus and $\rho(z)$ is the density of the plate, which are expressed as

$$E(z) = E_{\mathrm{m}} + (E_{\mathrm{c}} - E_{\mathrm{m}})\left(\frac{1}{2} - \frac{z}{h}\right)^n$$
$$\rho(z) = \rho_{\mathrm{m}} + (\rho_{\mathrm{c}} - \rho_{\mathrm{m}})\left(\frac{1}{2} - \frac{z}{h}\right)^n \tag{1}$$

where n is the power law index of FG rectangular plate, E_{m} is the Young modulus of metal surface, and E_{c} is the Young modulus of ceramic surface. Based on the classical plate theory, the displacement components are assumed to be

$$u_x(x, y, z, t) = u_0(x, y, t) - z\frac{\partial w_0(x, y, t)}{\partial x}$$
$$u_y(x, y, z, t) = v_0(x, y, t) - z\frac{\partial w_0(x, y, t)}{\partial y}$$
$$u_z(x, y, z, t) = w_0(x, y, t) \tag{2}$$

where u_0 and v_0 are the displacement of mid-plane in x- and y-directions, respectively; w_0 is the transverse displacement in the z-direction; and t is the time. Using the strain–displacement relations, the displacement components are defined as

$$\varepsilon_{xx} = \frac{\partial u_0}{\partial x} - z\frac{\partial^2 w_0}{\partial x^2}$$
$$\varepsilon_{yy} = \frac{\partial v_0}{\partial y} - z\frac{\partial^2 w_0}{\partial y^2}$$
$$2\varepsilon_{xy} = \frac{\partial u_0}{\partial y} + \frac{\partial v_0}{\partial x} - 2Z\frac{\partial^2 w_0}{\partial x \partial y} \tag{3}$$

Based on the Hooke's law for FG rectangular plates in plane stress state, the stress–strain relations are expressed as

$$\sigma_{xx} = \frac{E(z)}{1-\nu^2}(\varepsilon_{xx} + \nu\varepsilon_{yy})$$
$$\sigma_{yy} = \frac{E(z)}{1-\nu^2}(\varepsilon_{yy} + \nu\varepsilon_{xx})$$
$$\sigma_{xy} = \frac{E(z)}{2(1+\nu)}(2\varepsilon_{xy}) \tag{4}$$

where ν is the Poisson's ratio which is assumed to be a constant. By considering equations (2) and (3) and using the Hamilton's principle, the equations of motion for an FG rectangular plate are obtained as [**26**]

$$\frac{\partial N_{xx}}{\partial x} + \frac{\partial N_{xy}}{\partial y} = I_0\ddot{u}_0 - I_1\frac{\partial \ddot{w}_0}{\partial x}$$
$$\frac{\partial N_{xy}}{\partial x} + \frac{\partial N_{yy}}{\partial y} = I_0\ddot{v}_0 - I_1\frac{\partial \ddot{w}_0}{\partial y}$$
$$\frac{\partial^2 M_{xx}}{\partial x^2} + 2\frac{\partial^2 M_{xy}}{\partial x \partial y} + \frac{\partial^2 M_{yy}}{\partial y^2} = I_0\ddot{w}_0 + I_1\left(\frac{\partial \ddot{u}_0}{\partial x} + \frac{\partial \ddot{v}_0}{\partial y}\right) - I_2\left(\frac{\partial^2 \ddot{w}_0}{\partial x^2} + \frac{\partial^2 \ddot{w}_0}{\partial y}\right) \tag{5}$$

where N_{xx}, N_{yy}, and N_{xy} are the in-plane resultant forces, M_{xx}, M_{yy}, and M_{xy} are the resultant moments and I_0, I_1, and I_2 are mass parameters that are defined as

$$(N_{xx}, N_{yy}, N_{xy}) = \int_{-h/2}^{h/2} (\sigma_{xx}, \sigma_{yy}, \sigma_{xy})\,\mathrm{d}z$$
$$(M_{xx}, M_{yy}, M_{xy}) = \int_{-h/2}^{h/2} (\sigma_{xx}, \sigma_{yy}, \sigma_{xy})z\,\mathrm{d}z$$
$$(I_0, I_1, I_2) = \int_{-h/2}^{h/2} \rho(z)(1, z, z^2)\,\mathrm{d}z \tag{6}$$

By substituting equations (3) and (4) into equation (6), the resultant forces and moments are expressed in terms of displacement components as

$$N_{xx} = A_{11}\frac{\partial u_0}{\partial x} + A_{12}\frac{\partial v_0}{\partial y} - B_{11}\frac{\partial^2 w_0}{\partial x^2} - B_{12}\frac{\partial^2 w_0}{\partial y^2}$$
$$N_{yy} = A_{11}\frac{\partial v_0}{\partial y} + A_{12}\frac{\partial u_0}{\partial x} - B_{11}\frac{\partial^2 w_0}{\partial y^2} - B_{12}\frac{\partial^2 w_0}{\partial x^2}$$
$$N_{xy} = A_{33}\left(\frac{\partial u_0}{\partial y} + \frac{\partial v_0}{\partial y}\right) - 2B_{33}\left(\frac{\partial^2 w_0}{\partial x \partial y}\right)$$
$$M_{xx} = B_{11}\frac{\partial u_0}{\partial x} + B_{12}\frac{\partial v_0}{\partial y} - D_{11}\frac{\partial^2 w_0}{\partial x^2} - D_{12}\frac{\partial^2 w_0}{\partial y^2}$$
$$M_{yy} = B_{11}\frac{\partial v_0}{\partial y} + B_{12}\frac{\partial u_0}{\partial x} - D_{11}\frac{\partial^2 w_0}{\partial y^2} - D_{12}\frac{\partial^2 w_0}{\partial x^2}$$
$$M_{xy} = B_{33}\left(\frac{\partial u_0}{\partial y} + \frac{\partial v_0}{\partial y}\right) - 2D_{33}\left(\frac{\partial^2 w_0}{\partial x \partial y}\right) \tag{7}$$

where the parameters A_{ij}, B_{ij}, and D_{ij} are defined as

$$(A_{11}, B_{11}, D_{11}) = \int_{-h/2}^{h/2} \frac{E(z)}{1-\nu^2}(1, z, z^2)\,\mathrm{d}z$$
$$(A_{12}, B_{12}, D_{12}) = \int_{-h/2}^{h/2} \frac{\nu E(z)}{1-\nu^2}(1, z, z^2)\,\mathrm{d}z$$
$$(A_{33}, B_{33}, D_{33}) = \int_{-h/2}^{h/2} \frac{E(z)}{2(1+\nu)}(1, z, z^2)\,\mathrm{d}z \tag{8}$$

By substituting resultant forces and moments obtained from equation (7) into equation (5), the governing equations of motion for an FG rectangular plate are obtained as

$$A_{11}\left(\frac{\partial^2 u_0}{\partial x^2} + \frac{\partial^2 v_0}{\partial x \partial y}\right) + A_{33}\left(\frac{\partial^2 u_0}{\partial y^2} - \frac{\partial^2 v_0}{\partial x \partial y}\right) - B_{11}\left(\frac{\partial^3 w_0}{\partial x^3} + \frac{\partial^3 w_0}{\partial x \partial y^2}\right) = I_0\ddot{u}_0 - I_1\frac{\partial \ddot{w}_0}{\partial x}$$
$$A_{11}\left(\frac{\partial^2 v_0}{\partial y^2} + \frac{\partial^2 u_0}{\partial x \partial y}\right) + A_{33}\left(\frac{\partial^2 v_0}{\partial x^2} - \frac{\partial^2 u_0}{\partial x \partial y}\right) - B_{11}\left(\frac{\partial^3 w_0}{\partial y^3} + \frac{\partial^3 w_0}{\partial y \partial x^2}\right) = I_0\ddot{v}_0 - I_1\frac{\partial \ddot{w}_0}{\partial y}$$
$$B_{11}\left(\frac{\partial^3 u_0}{\partial x^3} + \frac{\partial^3 v_0}{\partial y^3} + \frac{\partial^3 v_0}{\partial x^2 \partial y} + \frac{\partial^3 u_0}{\partial x \partial y^2}\right) - D_{11}\left(\frac{\partial^4 w_0}{\partial x^4} + \frac{\partial^4 w_0}{\partial y^4} + 2\frac{\partial^4 w_0}{\partial x^2 \partial y^2}\right) = I_0\ddot{w}_0 + I_1\left(\frac{\partial \ddot{u}_0}{\partial x} + \frac{\partial \ddot{v}_0}{\partial y}\right) - I_2\left(\frac{\partial^2 \ddot{w}_0}{\partial x^2} + \frac{\partial^2 \ddot{w}_0}{\partial y^2}\right) \tag{9}$$

Equation (9) consists of three highly coupled partial differential equations in terms of the in-plane and transverse displacements. For solving these equations, it is reasonable to find a method for decoupling them. Equation (9) can be rewritten as

$$A_{11}\frac{\partial \phi_1}{\partial x} + A_{33}\frac{\partial \phi_2}{\partial y} - B_{11}\frac{\partial}{\partial x}(\nabla^2 w_0) = I_0\ddot{u}_0 - I_1\frac{\partial \ddot{w}_0}{\partial x} \tag{10a}$$
$$A_{11}\frac{\partial \phi_1}{\partial y} - A_{33}\frac{\partial \phi_2}{\partial x} - B_{11}\frac{\partial}{\partial y}(\nabla^2 w_0) = I_0\ddot{v}_0 - I_1\frac{\partial \ddot{w}_0}{\partial y} \tag{10b}$$
$$B_{11}\nabla^2\phi_1 - D_{11}\nabla^2\nabla^2 w_0 = I_0\ddot{w}_0 + I_1\ddot{\phi}_1 - I_2\nabla^2\ddot{w}_0 \tag{10c}$$

where ∇^2 is the Laplace operator and the variables ϕ_1 and ϕ_2 are defined as

$$\phi_1 = \frac{\partial u_0}{\partial x} + \frac{\partial v_0}{\partial y}$$
$$\phi_2 = \frac{\partial u_0}{\partial y} - \frac{\partial v_0}{\partial x} \tag{11}$$

Differentiating equations (10a) and (10b) with respect to x and y and doing some algebraic operations, one obtains

$$A_{11}\nabla^2\phi_1 - B_{11}\nabla^4 w_0 = I_0\ddot{\phi}_1 + I_1\nabla^2\ddot{w}_0 \tag{12a}$$
$$A_{33}\nabla^2\phi_2 - I_0\ddot{\phi}_2 = 0 \tag{12b}$$

By considering equations (12a) and (10c) and doing some algebraic processing, it can be shown that

$$\ddot{\phi}_1 = \frac{1}{(I_1 - (B_{11}/A_{11})I_0)}\left[\left(\frac{B_{11}^2}{A_{11}} - D_{11}\right)\nabla^4 w_0 + \left(I_2 - \frac{B_{11}I_1}{A_{11}}\right)\nabla^2\ddot{w}_0 - I_0\ddot{w}_0\right] \tag{13}$$

By substituting equation (13) into equation (12a), it is easy to show that

$$\hat{D}\nabla^6 w_0 + \left(\frac{B_{11}}{A_{11}}J_1 - \frac{\hat{D}I_0}{A_{11}} - J_2\right)\nabla^4\ddot{w} + \left(\frac{I_0J_2}{A_{11}} - \frac{I_1J_1}{A_{11}}\right)\nabla^2\ddddot{w}_0 + I_0\nabla^2\ddot{w}_0 - \frac{I_0^2}{A_{11}}\ddddot{w}_0 = 0 \tag{14}$$

where the parameters $\hat{D}, J_1$, and J_2 are defined as

$$\hat{D} = D_{11} - \frac{B_{11}^2}{A_{11}}$$
$$J_1 = I_1 - \frac{B_{11}I_0}{A_{11}}$$
$$J_2 = I_2 - \frac{B_{11}I_1}{A_{11}} \tag{15}$$

Therefore, by using the analytical method the equations of motion are converted into two decoupled equations (12b) and (14).

By using equations (10a) and (10b), the following relations can be found, which result in the in-plane displacement components

$$\ddot{u}_0 = \frac{1}{I_0}\left(A_{11}\frac{\partial\phi_1}{\partial x} + A_{33}\frac{\partial\phi_2}{\partial y} - B_{11}\frac{\partial}{\partial x}(\nabla^2 w_0) + I_1\frac{\partial\ddot{w}_0}{\partial x}\right)$$
$$\ddot{v}_0 = \frac{1}{I_0}\left(A_{11}\frac{\partial\phi_1}{\partial y} - A_{33}\frac{\partial\phi_2}{\partial x} - B_{11}\frac{\partial}{\partial y}(\nabla^2 w_0) + I_1\frac{\partial\ddot{w}_0}{\partial y}\right) \tag{16}$$

3 NAVIER SOLUTION

In this section, an FG simply supported rectangular plates is considered. Based on the Navier method, the transverse displacement w and function ϕ_2 are defined as

$$w(x, y) = \sum_{\kappa=1}^{\infty}\sum_{m=1}^{\infty} w_{m\kappa}\sin(\beta_m x)\sin(\eta_\kappa y)\mathrm{e}^{\mathrm{i}\omega_{m\kappa}t}$$
$$\phi_2(x, y) = \sum_{\kappa=1}^{\infty}\sum_{m=1}^{\infty} \phi_{m\kappa}\cos(\beta_m x)\cos(\eta_\kappa y)\mathrm{e}^{\mathrm{i}\omega_{m\kappa}t} \tag{17}$$

where β_m and η_κ are denoted by $m\pi/a$ and $\kappa\pi/b$, respectively. Also $\omega_{m\kappa}$ is the natural frequency. By substituting equation (17) into equations (14) and (12), the natural frequencies for simply supported rectangular plate can be obtained

$$\omega_{\mathrm{ss}1} = -\frac{\sqrt{2}}{2\beta_1}\sqrt{\chi_1(-\chi_2 + \sqrt{\chi_2^2 - 4\chi_1\chi_3})}$$
$$\omega_{\mathrm{ss}2} = -\frac{\sqrt{2}}{2\beta_1}\sqrt{-\chi_1(\chi_2 + \sqrt{\chi_2^2 - 4\chi_1\chi_3})}$$
$$\omega_{\mathrm{ss}3} = \frac{1}{I_0}\sqrt{I_0A_{33}(\beta_m^2 + \eta_n^2)} \tag{18}$$

The fundamental frequency for simply supported FG rectangular plate is the smallest value of above frequencies ($\omega_{\mathrm{ss}1}$). Also, the variables χ_j ($j = 1\ldots3$) are defined as

$$\chi_1 = (I_1^2 - I_0I_2)(\beta_m^2 + \eta_\kappa^2) - I_0^2$$
$$\chi_2 = (\eta_\kappa^4 + 2\eta_\kappa^2\beta_m^2 + \beta_m^4)(I_0D_{11} + I_2A_{11} - 2B_{11}I_1) + I_0A_{11}(\beta_m^2 + \eta_\kappa^2)$$
$$\chi_3 = (B_{11}^2 - A_{11}D_{11})(\beta_m^6 + 3\beta_m^4\eta_\kappa^2 + 3\beta_m^2\eta_\kappa^4 + \eta_\kappa^6) \tag{19}$$

Therefore, by considering the closed form (18) it is easy to obtain the natural frequency of simply supported FG rectangular plates.

4 LEVY SOLUTION

In this section, the free vibration analysis of FG rectangular plates with Levy boundary conditions is studied. It is assumed that the edges of the plate at $x = 0$ and a are simply supported; therefore, the solutions are considered as

$$w(x, y, z, t) = \sum_{m=1}^{\infty} w_m(y)\sin(\beta_m x)\mathrm{e}^{\mathrm{i}\omega_m t}$$
$$\phi_2(x, y, z, t) = \sum_{m=1}^{\infty} \phi_m(y)\cos(\beta_m x)\mathrm{e}^{\mathrm{i}\omega_m t} \tag{20}$$

Substituting equation (20) into equations (12b) and (14) yields

$$\mu_1 \frac{\mathrm{d}^6 w_m}{\mathrm{d}y^6} + (\mu_2 - 3\mu_1\beta_m^2)\frac{\mathrm{d}^4 w_m}{\mathrm{d}y^4} + (3\mu_1\beta_m^4 - 2\mu_2\beta_m^2 + \mu_3)\frac{\mathrm{d}^2 w_m}{\mathrm{d}y^2} + (\mu_4 - \mu_3\beta_m^2 - \mu_1\beta_m^6 + \mu_2\beta_m^4)w_m(y) = 0 \tag{21a}$$

$$A_{33}\frac{\mathrm{d}^2\phi_m}{\mathrm{d}y^4} + (\omega_m^2 I_0 - A_{33}\beta_m^2)\phi_m = 0 \tag{21b}$$

Equations (21) consist of two ordinary differential equations whose solutions are

$$w_m(y) = c_1\sinh(\lambda_1 y) + c_2\cosh(\lambda_1 y) + c_3\sinh(\lambda_2 y) + c_4\cosh(\lambda_2 y) + c_5\sinh(\lambda_3 y) + c_6\cosh(\lambda_3 y) \tag{22a}$$

$$\phi_m(y) = c_7\sinh(\lambda_4 y) + c_8\cosh(\lambda_4 y) \tag{22b}$$

where c_j $(j = 1\ldots 8)$ are the eight unknown constants. The variables of λ_j $(j = 1\ldots 4)$ are expressed as

$$\begin{aligned}
\lambda_1 &= \frac{\sqrt{3}}{6a}\sqrt{\frac{-a^2T^2 + 12a^2\hat{D}\mu_2 - 4a^2\mu_1^2 - 4T\mu_1a^2 + 12T\hat{D}m^2\pi^2 - \sqrt{3}a^2T^2 i - 12i\sqrt{3}a^2\hat{D}\mu_2 + 4i\sqrt{3}a^2\mu_1^2}{\hat{D}T}}\\
\lambda_2 &= \frac{\sqrt{3}}{6a}\sqrt{\frac{-a^2T^2 + 12a^2\hat{D}\mu_2 - 4a^2\mu_1^2 - 4T\mu_1a^2 + 12T\hat{D}m^2\pi^2 - \sqrt{3}a^2T^2 i - 12i\sqrt{3}a^2\hat{D}\mu_2 + 4i\sqrt{3}a^2\mu_1^2}{\hat{D}T}}\\
\lambda_3 &= \frac{\sqrt{6}}{6a}\sqrt{\frac{a^2T^2 - 12a^2\hat{D}\mu_2 + 4a^2\mu_1^2 - 2\mu_1Ta^2 + 6T\hat{D}m^2\pi^2}{\hat{D}T}}\\
\lambda_4 &= \frac{\sqrt{A_{33}m^2\pi^2 - \omega_m^2 I_0 a^2}}{a\sqrt{A_{33}}}
\end{aligned} \tag{23}$$

and the parameters μ_j $(j = 1\ldots 3)$ and T are defined as

$$\begin{aligned}
\mu_1 &= -\omega_m^2\left(\frac{B_{11}}{A_{11}}J_1 - \frac{\hat{D}I_0}{A_{11}} - J_2\right)\\
\mu_2 &= \omega_m^2\left(\frac{I_0J_2\omega_m^2}{A_{11}} - \frac{I_1J_1\omega_m^2}{A_{11}} - I_0\right)\\
\mu_3 &= -\frac{I_0^2\omega_m^4}{A_{11}}\\
T &= (36\hat{D}\mu_1\mu_2 - 108\hat{D}^2\mu_3 - 8\mu_1^3 + 12\sqrt{3}\hat{D}\sqrt{4\hat{D}\mu_2^2 - \mu_2^2\mu_1^2 - 18\hat{D}\mu_1\mu_2\mu_3 + 27\hat{D}^2\mu_3^2 + 4\mu_3\mu_1^3})^{(1/3)}
\end{aligned} \tag{24}$$

The general solutions (22) are valid for real λ_j $(j = 1\ldots 4)$. If these parameters become imaginary, the corresponding terms sinh and cosh are converted to sin and cos.

5 BOUNDARY CONDITIONS

Six possible boundary conditions in y-direction are considered, which are combinations of simply supported, clamped, and free boundary conditions.

For simply supported edges, the boundary conditions can be rewritten as

$$w = M_{yy} = N_{yy} = u = 0 \tag{25}$$

For clamped boundary conditions, it can be written that

$$w = u = v = \frac{\mathrm{d}w}{\mathrm{d}y} = 0 \tag{26}$$

and the boundary conditions of free edges require

$$M_{yy} = N_{yy} = N_{xy} = V_{yy} - I_1\omega_n^2 v = 0 \tag{27}$$

where

$$V_{yy} = \frac{\partial M_{yy}}{\partial y} + 2\frac{\partial M_{xy}}{\partial x} \tag{28}$$

Applying arbitrary boundary conditions at two edges of the FG plate in y-direction, a system of six

Table 1 Properties of the FGM components

Material	Properties		
	E (N/m^2)	ν	ρ (kg/m^3)
Aluminium (Al)	70×10^9	0.3	2707
Alumina (Al_2O_3)	380×10^9	0.3	3800
Ti–6Al–4V	105.7×10^9	0.298	4429
Aluminium oxide	320.2×10^9	0.26	3750

Table 2 Comparison of the natural frequency, $\varpi = \omega a^2\sqrt{12\rho(1-\nu^2)/Eh^3}$ for all boundary conditions square plate ($a/b = 1$, $h/a = 0.005$)

		SSSS	SCSC	SFSF	SSSC	SCSF	SSSF
ω_{11}	Reference [**28**]	19.74	28.95	9.63	23.65	12.69	11.68
	Present	19.76	29.01	9.64	23.66	12.69	11.70
ω_{12}	Reference [**28**]	49.35	69.32	16.13	58.64	33.06	27.76
	Present	49.37	69.33	16.19	58.69	33.11	27.76
ω_{13}	Reference [**28**]	98.70	129.09	36.72	113.22	72.40	61.86
	Present	98.74	129.08	36.75	113.28	72.44	61.87

Table 3 Comparison of the natural frequency ω (Hz) for simply supported square Ti–Al–4V/aluminium oxide FG plate ($a/b = 0.4$, $h/a = 0.005$)

n	Mode	Present	Reference [**19**]	Reference [**28**]	Reference [**10**]
0	1	143.40	143.67	145.04	144.66
	2	358.42	360.64	362.61	360.53
2000	1	273.906	268.60	271.23	268.92
	2	685.003	674.38	678.06	669.40

homogeneous algebraic equations is obtained. Setting the determinant of coefficient matrix equal to zero, the natural frequencies of the plate can be determined.

6 NUMERICAL RESULTS AND DISCUSSION

In this section, the numerical results have been presented for FG rectangular plates with all possible six boundary conditions along the edges in y-direction. The material properties have been listed in Table 1.

To verify the accuracy of the formulations, a comparison study of the results is performed with those available in the literature. In Table 2, for the special case of $n = 0$, the frequencies of FG rectangular plate with various boundary conditions are compared with those reported by Leissa [**27**] for isotopic plates and a good agreement can be seen. Also, for the special case of simply supported FG plate, the obtained results are compared with those reported by some references in Table 3. It can be seen that there is good agreement between the results and the small differences are due to the variation of Poisson ratio.

Table 4 Fundamental frequency parameter $\bar{\beta} = \omega\pi^2(a^2/h)\sqrt{\rho_m/E_m}$ for simply supported FG rectangular plate ($h/a = 0.01$)

n	b/a	$m = 1$	$m = 2$	$m = 3$
0	1	115.8695(1,1)	289.7708(1,2)	463.4781(2,2)
	2	72.3942(1,1)	115.8695(2,1)	188.2637(3,1)
0.5	1	98.0136(1,1)	245.3251(1,2)	392.4425(2,2)
	2	61.3313(1,1)	98.0136(2,1)	159.3448(3,1)
1	1	88.3093(1,1)	221.0643(1,2)	353.6252(2,2)
	2	55.1205(1,1)	88.3093(2,1)	143.6239(3,1)
2	1	80.3517(1,1)	200.8793(1,2)	321.4069(2,2)
	2	50.0743(1,1)	80.3517(2,1)	130.6201(3,1)

Table 5 Fundamental frequency parameters $\bar{\beta} = \omega\pi^2(a^2/h)\sqrt{\rho_m/E_m}$ for SCSC FG rectangular plate ($h/a = 0.01$)

n	b/a	$m = 1$	$m = 2$	$m = 3$
0	1	170.0196(1,1)	321.4069(1,2)	555.2809(2,2)
	2	80.3517(1,1)	138.7717(2,1)	227.0810(3,1)
0.5	1	143.8179(1,1)	272.1090(1,2)	470.0770(2,2)
	2	67.9302(1,1)	117.4222(2,1)	192.3395(3,1)
1	1	129.6496(1,1)	245.1310(1,2)	423.6904(2,2)
	2	61.1372(1,1)	105.7770(2,1)	173.3191(1,3)
2	1	117.8104(1,1)	222.8111(1,2)	385.0672(2,2)
	2	55.7028(1,1)	96.2668(2,1)	157.5981(3,1)

Table 6 Fundamental frequency parameters $\bar{\beta} = \omega\pi^2(a^2/h)\sqrt{\rho_m/E_m}$ for SFSF FG rectangular plate ($h/a = 0.01$)

n	b/a	$m = 1$	$m = 2$	$m = 3$
0	1	56.4791(1,1)	94.7141(2,1)	215.6299(3,1)
	2	57.0614(1,1)	68.5125(2,1)	103.8362(3,1)
0.5	1	47.7452(1,1)	80.1576(2,1)	182.4411(3,1)
	2	48.3275(1,1)	58.0318(2,1)	87.9211(3,1)
1	1	43.0872(1,1)	72.2001(2,1)	164.3911(3,1)
	2	43.4753(1,1)	52.2092(2,1)	79.1872(3,1)
2	1	39.1666(1,1)	65.6400(2,1)	149.0583(3,1)
	2	39.5936(1,1)	47.5511(2,1)	72.0060(3,1)

Table 7 Fundamental frequency parameters $\bar{\beta} = \omega\pi^2(a^2/h)\sqrt{\rho_m/E_m}$ for SSSC FG rectangular plate ($h/a = 0.01$)

n	b/a	$m = 1$	$m = 2$	$m = 3$
0	1	138.7717(1,1)	303.3569(1,2)	505.5948(2,2)
	2	75.6937(1,1)	126.3502(2,1)	206.7019(3,1)
0.5	1	117.4222(1,1)	256.7762(1,2)	428.1544(2,2)
	2	64.2426(1,1)	106.9415(2,1)	175.0658(3,1)
1	1	105.7770(1,1)	231.3509(1,2)	385.8435(2,2)
	2	57.8377(1,1)	96.4609(2,1)	157.5981(3,1)
2	1	96.2668(1,1)	210.3895(1,2)	350.7139(2,2)
	2	52.5974(1,1)	87.5329(2,1)	143.4298(3,1)

Table 8 Fundamental frequency parameters $\bar{\beta} = \omega\pi^2(a^2/h)\sqrt{\rho_m/E_m}$ for SSSF FG rectangular plate ($h/a = 0.01$)

n	b/a	$m=1$	$m=2$	$m=3$
0	1	68.5125(1,1)	162.8384(2,1)	346.8322(2,2)
	2	60.3608(1,1)	86.5625(2,1)	138.5776(3,1)
0.5	1	58.0318(1,1)	137.9954(2,1)	293.6526(2,2)
	2	51.0447(1,1)	73.3646(2,1)	117.4222(3,1)
1	1	52.2092(1,1)	124.2152(2,1)	264.5396(2,2)
	2	45.9985(1,1)	65.9893(2,1)	105.7770(3,1)
2	1	47.5511(1,1)	112.9582(2,1)	251.9240(3,1)
	2	41.9226(1,1)	59.9727(2,1)	96.0727(3,1)

Table 9 Fundamental frequency parameters $\bar{\beta} = \omega\pi^2(a^2/h)\sqrt{\rho_m/E_m}$ for SSCF FG rectangular plate ($h/a = 0.01$)

n	b/a	$m=1$	$m=2$	$m=3$
0	1	74.3350(1,1)	194.0863(2,1)	369.9285(2,2)
	2	61.1372(1,1)	92.3851(2,1)	151.3873(3,1)
0.5	1	63.0780(1,1)	164.3911(2,1)	313.2553(2,2)
	2	51.8210(1,1)	78.2168(2,1)	128.0969(3,1)
1	1	56.6732(1,1)	148.0878(2,1)	282.2015(2,2)
	2	46.5807(1,1)	70.4533(2,1)	115.4813(3,1)
2	1	51.6270(1,1)	134.6959(2,1)	256.5821(2,2)
	2	42.3108(1,1)	64.0485(2,1)	105.0007(3,1)

The non-dimensional frequency parameter $\bar{\beta} = \omega\pi^2 a^2\sqrt{\rho_m/E_m}/h$ for an FG plate consisting of Al/Al_2O_3 materials is shown in Tables 4 to 9 for various values of FG index n. The thickness–length ratio $h/a = 0.01$ and aspect ratio $b/a = 1$ and 2 are considered. In these tables, the first three non-dimensional frequencies are shown and the numbers in parenthesis present the wave numbers in the x- and y-direction, respectively. The boundary conditions are identified according to the edges of the plate. The six possible boundary conditions for FG rectangular plate containing SCSC, SCSS, SCSF, SSSF, SSSS, and SFSF have been considered in which S, C, and F stand for simply supported, clamped, and free boundary conditions, respectively. For example SCSF denotes a plate with simply supported boundary conditions in x-direction and clamped and free boundary conditions in y-direction. Also, the mode number of the natural frequency is shown in parenthesis in front of the natural frequencies.

It is observed that the non-dimensional frequency decreases as the aspect ratio increases except for the FG plates with free edge. When one edge of the plate becomes longer, the stiffness of the rectangular plate decreases. However, when the edge of the rectangular plate is free, the free edge gets smaller and causes an increase in the frequency, especially in the lower modes.

Also, it can be seen that for a constant aspect ratio, the frequency parameter decreases for all modes as the power of FGM, n, increases. The reason is that with increasing the power of FGM, the stiffness of the plate decreases and results in a decrease in the natural frequency of the FG rectangular plate.

In the most published articles concerning the analytical approaches to find the natural frequencies of FG plates, the effects of in-plane displacements have been neglected (see e.g. references [**18**], [**29**], and [**30**]). To study the effects of in-plane displacements on natural frequency of the FG plates, a comparison has been investigated with the results reported by Hosseini-Hashemi *et al.* [**18**]. They used the first-order shear deformation theory and ignored the in-plane displacements. Table 10 shows this comparison for an FG rectangular plate with different boundary conditions.

Table 10 Effect of in-plane displacements on non-dimensional fundamental frequencies $\varpi = \omega h\sqrt{\rho_c/E_c}$ for different boundary conditions, some thickness–length ratio and power law index ($a/b = 1.5$)

		SSSS			SSSC			SCSC		
h/a	n	Present	Reference [**18**]	Difference (%)	Present	Reference [**18**]	Difference (%)	Present	Reference [**18**]	Difference (%)
0.05	0	0.024 19	0.023 92	1.116	0.032 06	0.031 29	2.402	0.042 465	0.040 76	4.015
	1	0.018 45	0.021 56	−16.856	0.024 455	0.026 67	−9.061	0.032 395	0.032 50	−0.324
	5	0.015 90	0.021 80	−37.107	0.021 070	0.026 77	−27.053	0.027 905	0.032 39	−16.072
0.1	0	0.095 800	0.091 88	4.09	0.126 840	0.116 39	8.238	0.167 930	0.145 80	13.178
	1	0.073 020	0.081 55	−11.682	0.096 66	0.097 34	−0.703	0.127 970	0.114 53	10.502
	5	0.062 810	0.081 71	−30.09	0.083 130	0.096 46	−16.035	0.110 040	0.112 34	−2.090
		SFSF			SCSF			SSSF		
h/a	n	Present	Reference [**18**]	Difference (%)	Present	Reference [**18**]	Difference (%)	Present	Reference [**18**]	Difference (%)
0.05	0	0.007 28	0.007 19	1.236	0.012 72	0.012 49	1.808	0.010 365	0.010 24	1.206
	1	0.005 55	0.006 74	−21.441	0.009 705	0.011 32	−16.641	0.007 910	0.009 48	−19.848
	5	0.004 79	0.006 85	−43.006	0.008 360	0.011 46	−37.081	0.006 815	0.009 63	−41.306
0.1	0	0.029 05	0.028 35	2.409	0.050 740	0.048 17	5.065	0.041 33	0.040 01	3.194
	1	0.022 16	0.026 41	−19.178	0.038 690	0.043 27	−11.837	0.031 520	0.036 79	−16.719
	5	0.019 09	0.026 77	−40.230	0.033 310	0.043 52	−30.651	0.027 140	0.037 18	−36.994

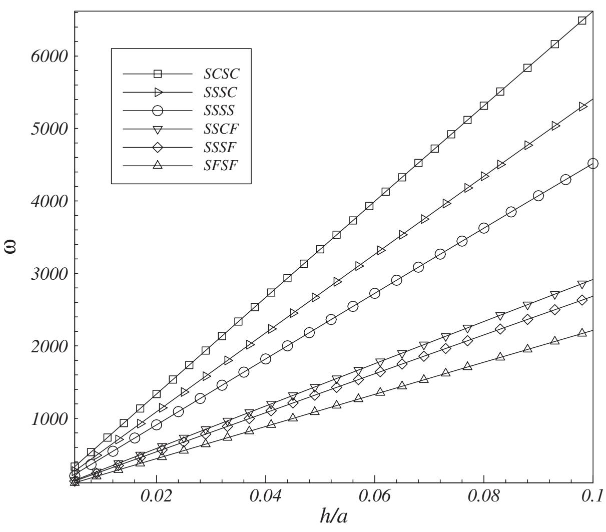

Fig. 2 First natural frequency of FG rectangular plate versus the thickness–length ratio for all boundary conditions ($n = 1, a/b = 1$)

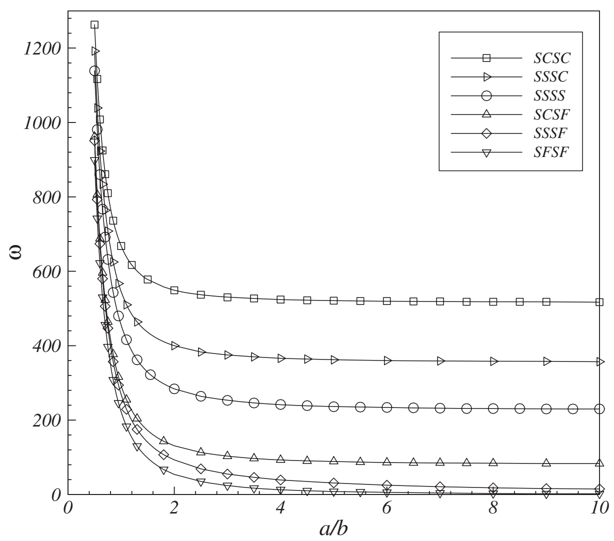

Fig. 3 First natural frequency of FG rectangular plate versus the aspect ratio for all boundary conditions ($n = 1, h/a = 0.01, a = 1$)

It can be seen that there are major differences between the results of the present work and those of reference [**18**]. Two reasons cause the differences. The first reason is because of the difference of the classical and first-order shear deformation plate theories. The second reason is due to the effects of in-plane displacements. For the case $n = 0$, the plate is a homogenous isotropic plate and therefore the in-plane displacements are ineffective on natural frequencies of the plate. Thus, in this case the differences are due to the first reason, which has a small effect on natural frequency of thin plates. It can be seen that for isotropic plates ($n = 0$), the difference is positive. This is due to the fact that the classical plate theory overestimates the natural frequency. From Table 10, it can be seen that for FG plates (i.e. $n > 0$), the difference is negative and its magnitude increases greatly with increasing the power law index n. In other words, the natural frequencies reported in reference [**18**], based on first-order shear deformation theory, are greater than those obtained in this study. This significant difference is because of neglecting the in-plane displacements in reference [**18**]. Thus, the in-plane displacements have a substantial role in natural frequencies of FG plates.

In order to find the effects of boundary conditions on the natural frequencies of the plate, variation of first natural frequency versus the variation of thickness–length ratio h/a is shown in Fig. 2. It can be concluded that more constrains at the edges of the FG plate increase natural frequency of the rectangular plate. Therefore, the SCSC plate has the highest and the SFSF rectangular plate has the lowest natural frequencies. Also, variation of first natural frequency versus the variation of aspect ratio a/b is depicted in Fig. 3 for different boundary conditions. It can be seen that for higher values of aspect ratio, the effect of boundary condition is more significant.

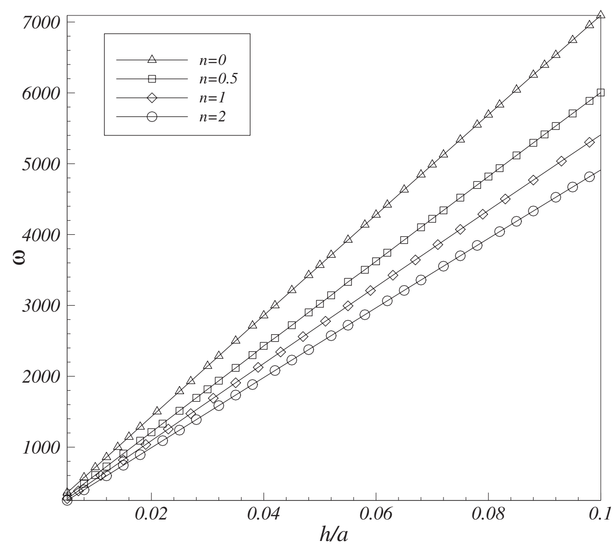

Fig. 4 First natural frequency of FG rectangular plate versus the thickness–length ratio for SSSC boundary condition ($a/b = 1$)

The variation of natural frequency versus the variation of thickness–length ratio is shown in Fig. 4 for different power law indexes. It can be concluded that as the thickness of the plate increases, the effect of non-homogeneity in the material properties of the plate on the natural frequency becomes more considerable. Also, the mode shape counter plates are shown for an FG rectangular plate for all possible boundary conditions along the y-direction in Fig. 5.

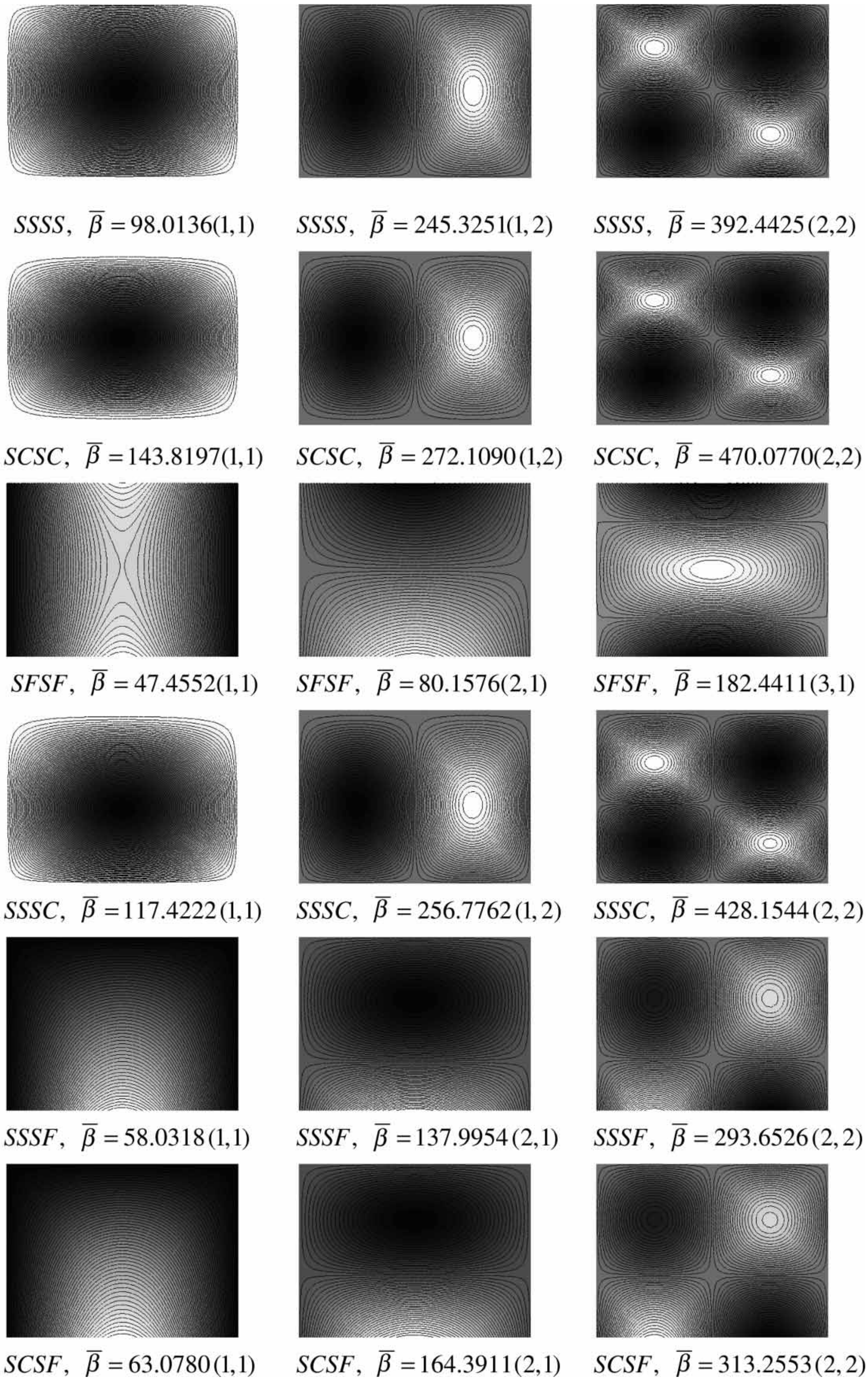

Fig. 5 Mode shape plots of the rectangular plate for various boundary conditions ($n = 0.5, h/a = 0.01, a/b = 1$)

7 CONCLUSION

The analytical solution has been presented for free vibration analysis of FG thin plates. Three coupled partial differential equations of motion have been reformulated into two decoupled equations. By using the Navier method, a closed-form solution for FG rectangular plates has been presented. The Levy approach has been used to find the natural frequencies of FG plates with different boundary conditions. Accurate non-dimensional frequency parameter has been tabulated for different boundary conditions, some powers of FGM, and aspect ratios. The following conclusions can be made.

1. The non-dimensional frequency decreases as the aspect ratio increases except for the FG plates with free edge.
2. For a constant aspect ratio, the frequency parameter decreases for all modes as the power of FGM (n) increases.
3. The in-plane displacements have a substantial role in natural frequencies of FG plates.
4. It can be seen that for higher values of the aspect ratio, the effect of boundary condition is more significant.
5. As the thickness of the plate increases, the effect of material non-homogeneity on the natural frequency becomes more considerable.

REFERENCES

1 **Koizumi, M.** FGM activities in Japan. *Compos. B*, 1997, **28**(1–2), 1–4.

2 **Chi, S.** and **Chung, Y.** Mechanical behavior of functionally graded material plates under transverse load. Part 1: analysis. *Int. J. Solids Struct.*, 2006, **43**, 3657–3674.

3 **Chi, S.** and **Chung, Y.** Mechanical behavior of functionally graded material plates under transverse load. Part 2: numerical results. *Int. J. Solids Struct.*, 2006, **43**, 3675–3691.

4 **Birman, V.** and **Byrd, L. W.** Modeling and analysis of functionally graded materials and structures. *ASME J. Appl. Mech.*, 2007, **60**, 195–216.

5 **Yang, J.** and **Shen, H. S.** Dynamic response of initially stressed functionally graded rectangular thin plates. *Compos. Struct.*, 2001, **54**, 497–508.

6 **Qian, L. F., Batra, R. C.,** and **Chen, L. M.** Static and dynamic deformations of thick functionally graded elastic plates by using higher-order shear and normal deformable plate theory and meshless local Petrov–Galerkin method. *Compos. B*, 2004, **35**, 685–697.

7 **Gilhooley, D. F., Batra, R. C., Xiao, J. R., McCarthy, M. A.,** and **Gillespie, J. W.** Analysis of thick functionally graded plates by using higher-order shear and normal deformable plate theory and MLPG method with radial basis functions. *Compos. Struct.*, 2007, **80**, 539–552.

8 **Ferreira, A. J. M., Batra, R. C., Roque, C. M. C., Qian, L. F.,** and **Martins, P. A. L. S.** Static analysis of functionally graded plates using third-order shear deformation theory and a meshless method. *Compos. Struct.*, 2005, **69**, 449–457.

9 **Ferreira, A. J. M., Batra, R. C., Roque, C. M. C., Qian, L. F.,** and **Jorge, R. M. N.** Natural frequencies of functionally graded plate by a meshless method. *Compos. Struct.*, 2006, **75**, 593–600.

10 **He, X. Q., Ng, T. Y., Sivashanker, S.,** and **Liew, K. M.** Active control of FGM plates with integrated piezoelectric sensors and actuators. *Int. J. Solids Struct.*, 2001, **38**, 1641–1655.

11 **Vel, S. S.** and **Batra, R. C.** Three-dimensional exact solution for the vibration of functionally graded rectangular plates. *J. Sound Vibr.*, 2004, **272**, 703–730.

12 **Malekzadeh, P.** Three-dimensional free vibration analysis of thick functionally graded plates on elastic foundations. *Compos. Struct.*, 2009, **89**, 367–373.

13 **Li, Q., Iu, V. P.,** and **Kou, K. P.** Three-dimensional vibration analysis of functionally graded material plates in thermal environment. *J. Sound Vibr.*, 2009, **324**, 733–750.

14 **Kim, Y. W.** Temperature dependent vibration analyses of functionally graded rectangular plates. *J. Sound Vibr.*, 2005, **284**, 531–549.

15 **Matsunaga, H.** Free vibration and stability of functionally graded plates according to a 2-D higher-order deformation theory. *Compos. Struct.*, 2008, **82**, 499–512.

16 **Zhang, D. G.** and **Zhou, Y. H.** A theoretical analysis of FGM thin plates based on physical neutral surface. *Comput. Mater. Sci.*, 2008, **44**, 716–720.

17 **Fares, M. E., Elmarghany, M. K.,** and **Atta, D.** An efficient and simple refined theory for bending and vibration of functionally graded plates. *Compos. Struct.*, 2009, **91**, 296–305.

18 **Hosseini-Hashemi, S., Rokni Damavandi Taher, H., Akhavan, H.,** and **Omidi, M.** Free vibration of functionally graded rectangular plates using first-order shear deformation plate theory. *Appl. Math. Model.*, 2010, **34**, 1276–1291.

19 **Zhao, X., Lee, Y. Y.,** and **Liew, K. M.** Free vibration analysis of functionally graded plates using the element-free *kp*-Ritz method. *J. Sound Vibr.*, 2009, **319**, 918–939.

20 **Liu, D. Y., Wang, C. Y.,** and **Chen, W. Q.** Free vibration of FGM plates with in-plane material inhomogeneity. *Compos. Struct.*, 2010, **92**, 1047–1051.

21 **Jomehzadeh, E.** and **Saidi, A. R.** Analytical solution for free vibration of transversely isotropic sector plates using a boundary layer function. *Thin-Walled Struct.*, 2009, **47**, 82–88.

22 **Jomehzadeh, E.** and **Saidi, A. R.** Accurate natural frequencies of transversely isotropic moderately thick annular sector plates. *Proc. IMechE, Part C: J. Mechanical Engineering Science*, 2009, **223**, 307–317. DOI: 10.1243/09544062JMES1199.

23 **Saidi, A. R.** and **Jomehzadeh, E.** On analytical approach for the bending/stretching of linearly elastic functionally graded rectangular plates with two opposite edges simply supported. *Proc. IMechE, Part C: J. Mechanical Engineering Science*, 2009, **223**, 2009–2016. DOI: 10.1243/09544062JMES1431.

24 **Mohammadi, M., Saidi, A. R.,** and **Jomehzadeh, E.** Levy solution for buckling analysis of functionally graded rectangular plates. *Appl. Compos. Mater.*, 2010, **17**, 81–93.

25 **Mohammadi, M., Saidi, A. R.,** and **Jomehzadeh, E.** A novel analytical approach for buckling analysis of moderately thick functionally graded rectangular plates with two opposite edges simply supported. *Proc. IMechE, Part C: J. Mechanical Engineering Science*, 2009, in press. DOI: 10.1243/09544062JMES1804.

26 **Reddy, J. N.** *Theory and analysis of elastic plates*, 1999 (Taylor & Francis, Philadelphia).

27 **Leissa, A. W.** Vibration of plates. NASA report SP-160, Washington, DC, 1969.
28 **Bishop, R. E. D.** *The mechanics of vibration*, 1979 (Cambridge University Press, New York).
29 **Ebrahimi, F., Rastgoo, A.,** and **Atai, A. A.** A theoretical analysis of smart moderately thick shear deformable annular functionally graded plate. *Eur. J. Mech. A, Solids*, 2009, **28**, 962–973.
30 **Ebrahimi, F.** and **Rastgoo, A.** An analytical study on the free vibration of smart circular thin FGM plate based on classical plate theory. *Thin-Walled Struct.*, 2008, **46**, 1402–1408.